Activation of the μ Opioid Receptor Involves Conformational Rearrangements of Multiple Transmembrane Domains[†]

Wei Xu,[‡] Arantxa Sanz,[§] Leonardo Pardo,[§] and Lee-Yuan Liu-Chen*,[‡]

Department of Pharmacology and Center for Substance Abuse Research, Temple University School of Medicine, Philadelphia, Pennsylvania 19140, and Laboratori de Medicina Computacional, Unitat de Bioestadística, Universitat Autònoma de Barcelona, Barcelona, Spain

ABSTRACT: We previously demonstrated that D3.49(164)Y or T6.34(279)K mutation in the rat μ opioid receptor (MOPR) resulted in agonist-independent activation. Here, we identified the cysteine(s) within the transmembrane domains (TMs) of the D3.49(164)Y mutant that became accessible in the binding-site crevice by use of methanethiosulfonate ethylammonium (MTSEA) and inferred conformational changes associated with receptor activation. While the C7.38(321)S mutant was insensitive to MTSEA, the D3.49(164)Y/C7.38(321)S mutant showed similar sensitivity as the D3.49(164)Y, suggesting that, in the D3.49(164)Y mutant, C7.38(321) becomes inaccessible while other cysteines are accessible in the binding-site crevice. Each of the other seven cysteines in the TMs was mutated to serine on the background of D3.49(164)Y/C7.38(321)S, and the resulting triple mutants were evaluated for [3H]diprenorphine and [D-Ala2,NMe-Phe4,Gly5-ol]-enkephalin (DAMGO) binding and effect of MTSEA on [3H]diprenorphine binding. The D3.49(164)Y/C7.38(321)S mutant and the triple mutants, except the C6.47(292)S triple mutant, retained similar affinities for [3H]diprenorphine and DAMGO as the D3.49(164)Y mutant. The second-order rate constants for MTSEA reactions showed that C3.44(159)S, C4.48(190)S, C5.41(235)S, and C7.47(330)S significantly reduced sensitivity to MTSEA, compared with the D3.49(164)Y/C7.38(321)S. These results suggest that the four cysteines may be rotated and/or tilted to become accessible. While the D3.49(164)Y/C7.38(321)S was similarly sensitive to MTSEA as the D3.49(164)Y mutant, the T6.34(279)K/C7.38(321)S was much less sensitive to MTSEA than the T6.34(279)K mutant, suggesting that the two constitutively active mutants assume different conformations and/or possess different dynamic properties. Molecular models of the MOPR monomer and homodimer, using the crystal structures of rhodopsin, the β_2-adrenergic receptor, and the ligand-free opsin, which contains several features characteristic of the active state, were employed to analyze these experimental results in a structural context.

Opioid receptors (μ, δ, and κ) belong to the rhodopsin subfamily of seven-transmembrane domain receptors (7TMRs)[1]. According to various models, 7TMRs exist in equilibrium between activated and inactive states, and agonists shift the equilibrium in favor of activated states. The detailed mechanisms underlying the conformational changes from inactive states to activated states of 7TMRs are emerging (see reviews in refs 1–3 and references cited therein). Disruption of interactions among TMs has been implicated in receptor activation. In the high-resolution

crystal structure of the inactive form of rhodopsin (4), the interactions between R3.50(135) and the preceding E3.49(134) as well as with E6.30(247) and T6.34(251) in TM6 are evident. Mutations that interfere with the interactions between these or corresponding residues in TM3 and TM6 resulted in constitutive activation of rhodopsin and β_2-adrenergic and μ opioid receptors. Notably, in the structures of the inactive forms of the β_1- and β_2-adrenergic receptors (5–8) the ionic interaction between R3.50 with the adjacent D3.49 in TM3 is maintained, but the interaction with E6.30 in TM6 is not observed, which may be responsible for the relatively high basal activity. The recent crystal structure of the ligand-free opsin shows an intracellular part of TM6 tilted outward by 6–7 Å, while R3.50 adopts an extended conformation pointing toward the protein core (9). Binding of Zn^{2+} to substituted histidines at the cytoplasmic ends of TM3 and TM6, preventing movements of the two TMs, blocks activation of rhodopsin and β_2-adrenergic and parathyroid hormone receptors. Interference of an ionic interaction between a negatively charged residue in TM3 and a positively charged residue in TM7 in rhodopsin and α_{1b}-adrenergic and δ opioid receptors leads to activation of the receptors. Blockade of movements of extracellular ends of TM5 and TM6 abolished activation of the neurokinin NK-1

* To whom correspondence should be addressed. Phone: (215) 707-4188. Fax: (215) 707-7068. E-mail: lliuche@temple.edu.
‡ Temple University School of Medicine.
§ Universitat Autònoma de Barcelona.

1 Abbreviations: 7TMR, seven-transmembrane domain receptor; ANOVA, *an*alysis *of v*ariance; CAM, constitutively active mutant; DAMGO, [D-Ala2,NMe-Phe4,Gly5-ol]-enkephalin; Kreb's solution, NaCl, 130 mM; KCl, 4.8 mM; KH_2PO_4, 1.2 mM; $CaCl_2$, 1.3 mM; $MgSO_4$, 1.2 mM; glucose, 10 mM; and HEPES, 25 mM, pH 7.4; MD, molecular dynamics; MOPR, μ opioid receptor; MTS, methanethiosulfonate; MTSEA, methanethiosulfonate ethylammonium; PCR, polymerase chain reaction; RMOPR, rat μ opioid receptor; TM, transmembrane domain; WT, wild type.

receptor. In addition, elimination of aromatic−aromatic interactions between Y7.63 in TM7 and F7.60 in helix 8 in the NPXXYX$_{5,6}$F motif was suggested to be important for the activation of rhodopsin and 5-hydroxytryptamine$_{2C}$ receptor. Moreover, the highly conserved N7.49 is thought to act as the on/off switch. In the inactive state, N7.49 is constrained toward TM6 by intramolecular interactions, and upon activation, N7.49 is suggested to adopt *trans* conformations and react with D2.50 in TM2.

We reported previously that in the MOPR mutation of the D3.49(164) to H, Q, Y or M in the highly conserved DRY motif in the TM3 or substitution of T6.34(279) with Lys at the junction of the i3 loop and the TM6 led to agonist-independent activation (*10, 11*). These mutants thus can be used to elucidate conformational changes associated with activation of the receptor.

Methanethiosulfonate ethylammonium, $CH_3SO_2SCH_2CH_2$-NH_3^+ (MTSEA), is one of the small and charged methanethiosulfonate (MTS) reagents developed by Karlin and colleagues (*12*) that react specifically with reduced sulfhydryl groups. When reacted with cysteine, $-SCH_2CH_2NH_3^+$ of MTSEA forms mixed disulfide bonds with the $-SH$ group of cysteine. Since MTS reagents react 10^9 times faster with ionized thiolates than with un-ionized thiols and ionization of cysteine is likely to occur to a significant extent only for water-accessible residues, their reaction rates with cysteine residues would be expected to be highest with water-accessible cysteines and much less with those in the interior of proteins or facing lipid. Binding pockets of 7TMRs in the rhodopsin subfamily are formed by the seven TMs and are accessible to the extracellular medium. Within the binding pocket, water-accessible residues can directly interact with ligands. Reaction of MTSEA with cysteine residues in the binding pocket often interferes with ligand binding. Javitch and colleagues used the MTS reagents to identify Cys3.36(118) being exposed in the binding-site crevice of the D$_2$ dopamine receptor and to map the residues accessible in the binding-site crevice of the same receptor with the substituted cysteine accessibility method (SCAM) (for a review, see ref *13*). We have shown that reaction with MTSEA reduces [³H]diprenorphine to the μ receptor, and this sensitivity is mostly attributed to its reaction with C7.38(321) (*14*), indicating that C7.38(321) is exposed in the binding-site crevice. In addition, we used SCAM to compare residues exposed in the binding-site crevices in the TM7 of the μ, δ, and κ opioid receptors (*15*) and in the TM6 of the δ and κ receptors (*16*).

In this study, we examined the effect of MTSEA on [³H]diprenorphine binding to the constitutive active D3.49-(164)Y mutant of the MOPR and determined the cysteine residue(s) that conferred the MTSEA reactivity, thereby identifying the cysteine residues within TMs that became accessible in the binding-site crevice of the mutant. We then inferred from the experimental data the changes in TMs that may occur during activation of the MOPR by molecular modeling.

MATERIALS AND METHODS

Materials. [³H]Diprenorphine (58 Ci/mmol) was purchased from Perkin-Elmer Life Sciences (Boston, MA). Naloxone was a gift from the former DuPont Pharmaceutical Co. (Wilmington, DE). MTS reagents were purchased from Toronto Research Chemicals (North York, Ontario, Canada).

Enzymes and chemicals used in molecular biology and mutagenesis experiments were purchased from Life Technologies Co. (Gaithersburg, MD), Promega (Madison, WI), Bohringer-Mannheim Co. (Indianapolis, IN), and Qiagen Co. (Valencia, CA).

Numbering Schemes for Amino Acid Residues in Opioid Receptors. Two numbering schemes were used. Amino acid residues in the rat MOPR were identified by their sequence numbers. In addition, the generic numbering scheme of amino acid residues in 7TMRs proposed by Ballesteros and Weinstein (*17*) was used in order to relate the results to equivalent positions in other 7TMRs. According to the generic numbering scheme, amino acid residues in TMs are assigned two numbers (N1.N2). N1 refers to the TM number. For N2, the numbering is relative to the most conserved residue in each TM, which is assigned 50; the other residues in the TM are numbered in relation to this conserved residue, with numbers decreasing toward the N-terminus and increasing toward the C-terminus. The generic numbering has been applied to opioid receptors (for example, refs *14−16*), which allows for cross-reference to published literature on other 7TMRs.

Oligodeoxynucleotide-Directed Mutagenesis. Site-directed mutagenesis was performed on the rat μ receptor with the overlap polymerase chain reaction (PCR) method described previously (*14*). Three single mutants of the rat μ opioid receptors, C7.38(321)S, D3.49(164)Y, and T6.34(279)K, were generated previously (*10, 11, 14*). The double mutants D3.49(164)Y/C7.38(321)S and T6.34(279)K/C7.38(321)S were constructed on the background D3.49(164)Y and T6.34(279)K, respectively, with the overlap PCR method and subcloned into the *Hin*dIII site of the mammalian expression vector pcDNA3, and the clones with the right orientation were identified with *Bam*HI digestion. There are eight native cysteine residues in the TMs of the rat MOPR (Figure 1). Each cysteine residue in the TMs was mutated to serine one at a time on the background of the double mutant D3.49(164)Y/C7.38(321)S, resulting in seven triple mutants: C1.49(79)S, C3.44(159)S, C4.48(190)S, C5.41(235)S, C5.57(251)S, C6.47(292)S, C7.47(330)S. DNA sequence was determined to confirm the presence of desired mutations and the absence of unwanted mutations.

Cell Culture and Transfection. HEK293 cells were grown in 100 mm culture dishes in minimum essential medium supplemented with 10% fetal calf serum, 100 units/mL penicillin, and 100 μg/mL streptomycin in a humidified atmosphere consisting of 5% CO_2 and 95% air at 37 °C. Cells were transfected with the cDNA of the WT or a mutant of the rat MOPR (8 μg/dish) using the lipofectamine method as described previously (*14*). The D3.49(164)Y, T6.34(279)K, T6.34(279)K/C7.38(321)S, and D3.49(164)Y/C7.38(321)S and all the triple mutants were pretreated with naloxone (20 μM) for 24 h to enhance expression levels. After transfection (60−72 h), cells were detached by use of Kreb's solution (NaCl, 130 mM; KCl, 4.8 mM; KH$_2$PO$_4$, 1.2 mM; CaCl$_2$, 1.3 mM; MgSO$_4$, 1.2 mM; glucose, 10 mM; and HEPES, 25 mM; pH 7.4), pelleted at 1000g for 1 min at room temperature, and washed three times with Kreb's buffer by centrifugation and resuspension to remove serum and naloxone.

Opioid Receptor Binding in Intact Cells. Binding was carried out as described previously (*14*). Saturation binding of [³H]diprenorphine to the rat μ WT and mutant receptors

Rat μ opioid receptor
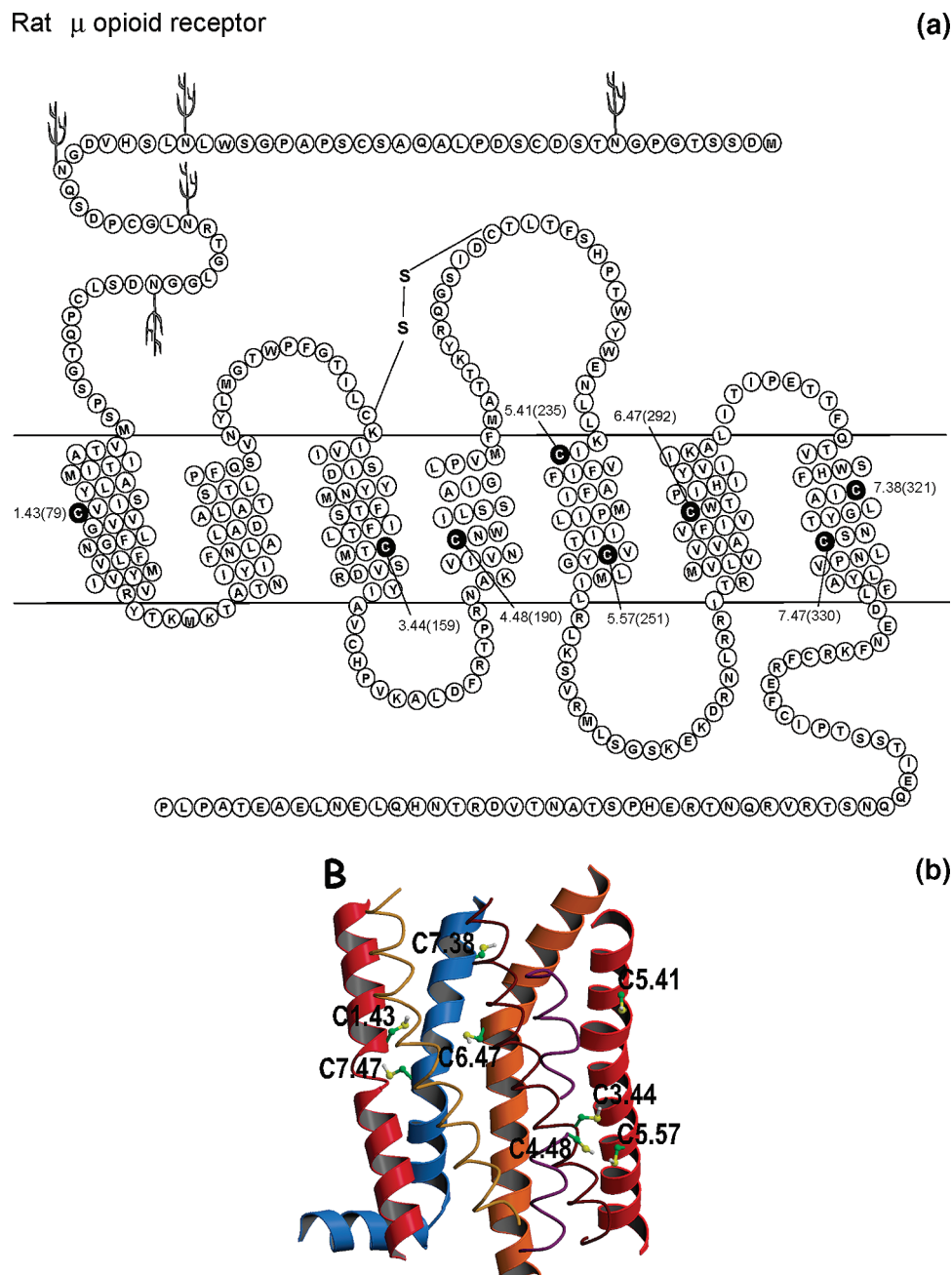
(a)

B

(b)

FIGURE 1: (A) Schematic representation of amino acid sequences of the rat MOPR and cysteine residues within the putative transmembrane domains. The single letter amino acid codes are used for the amino acid sequences. The dark circles indicate cysteine residues in the transmembrane domains. The numbers refer to the positions of the residues within the protein sequences. (B) Positions of C1.43(79), C3.44(159), C4.48(190), C5.41(235), C5.57(251), C6.47(292), C7.38(321), and C7.47(330) in a molecular model of transmembrane helices 1 (crimson), 2 (goldenrod), 3 (dark red), 4 (magenta), 5 (red), 6 (orange), and 7 (blue) of the μ opioid receptor.

was performed on intact cells with at least six concentrations of [³H]diprenorphine (ranging from 25 pM to 2 nM), and K_d and B_{max} values were determined. Competition inhibition by DAMGO of [³H]diprenorphine binding to the WT and mutant receptors was performed with 0.3 nM [³H]diprenorphine in the absence or presence of increased concentrations of DAMGO, and the K_i value of DAMGO was determined. Binding was carried out in Kreb's solution at room temperature for 1 h in duplicate in a volume of 1 mL with about 10⁶ cells. Naloxone (10 μM) was used to define nonspecific binding. Binding data were analyzed with the Prism program (GraphPad Software Inc., San Diego, CA).

Reaction with MTSEA. The experiments were performed as described previously (*14*). The cell pellets were resus-

pended in Kreb's solution, and aliquots of the cell suspension were incubated without (control) or with freshly prepared MTSEA at the stated concentration in a final volume of 0.5 mL at room temperature for 5 min. The reaction was stopped by adding 0.5 mL of 0.8% BSA solution. After centrifugation, the pellet were resuspended in 1 mL/dish Kreb's solution, and 200 μL aliquots were used for [³H]diprenorphine binding. The fractional inhibition was calculated as [1 − (specific binding with MTSEA treatment/specific binding without the reagent)] × 100.

Determination of Second-Order Rate Constants. The second-order rate constant of interaction between the WT and the mutants and MTSEA was determined to gain quantitative information on MTSEA sensitivity, as described

Table 1: K_d and B_{max} Values of [3H]Diprenorphine Binding and Apparent K_i Values of DAMGO Binding to Wild Type (WT) and Mutants of Rat μ Opioid Receptors Transiently Expressed in HEK293 Cells[a]

constructs	[3H]diprenorphine		DAMGO		
	K_d (nM)	B_{max} (pmol/10^6 cell)	K_i (nM)	D3.49Y/mutant	WT/mutant
RMOPR WT	0.19 ± 0.05	0.43 ± 0.01	432 ± 79.6[b]		1
C7.38(321)S	0.14 ± 0.01	0.11 ± 0.01	237 ± 26.8[b]		2
D3.49(164)Y	0.25 ± 0.01	0.17 ± 0.01	88 ± 12.7	1	5
D3.49Y/C7.38S	0.31 ± 0.02	0.69 ± 0.04	59 ± 8.4	1.5	7
C1.49(79)S/D3.49Y/C7.38S	0.23 ± 0.02	0.12 ± 0.01	46 ± 8.7	1.9	9
C3.44(159)S/D3.49Y/C7.38S	0.24 ± 0.01	0.10 ± 0.001	39 ± 12.9	2.3	11
C4.48(190)S/D3.49Y/C7.38S	0.17 ± 0.01	0.26 ± 0.006	18 ± 3.4	4.9	24
C5.41(235)S/D3.49Y/C7.38S	0.22 ± 0.01	0.17 ± 0.008	65 ± 11.9	1.4	7
C5.57(251)S/D3.49Y/C7.38S	0.18 ± 0.01	0.22 ± 0.006	29 ± 12.6	3.0	15
C6.47(292)S/D3.49Y/C7.38S	NB				
C7.47(330)S/D3.49Y/C7.38S	0.23 ± 0.003	0.29 ± 0.004	110 ± 15.7	0.8	4
T6.34(279)K	0.17 ± 0.02	0.22 ± 0.01	6.3 ± 1.1		69
T6.34K/C7.38S	0.24 ± 0.003	0.35 ± 0.01	10 ± 0.9		43

[a] Saturation binding of [3H]diprenorphine to the wt or mutant receptor was performed on intact cells, and K_d and B_{max} values were determined. Competitive inhibition of [3H]diprenorphine binding to the wt or mutant receptor by DAMGO was carried out on intact cells, and IC_{50} values were determined. Apparent K_i values were calculated according to the equation $K_i = IC_{50}/(1 + [L]/K_d)$. Each value represents the mean ± SEM of three to six independent experiments performed in duplicate. [b] $P < 0.01$, compared with the D3.49(164)Y by one-way ANOVA followed by the post hoc Dunnett multiple comparison test.

previously (14). Each receptor was incubated with four indicated concentrations of MTSEA for 5 min. The results were fit to the equations:

$$Y = (\text{extent of inhibition})e^{-kct} + \text{plateau}$$

$$\text{extent of inhibition} + \text{plateau} = 1.0$$

Y is the fraction of the initial binding, k is the second-order rate constant ($M^{-1}\ s^{-1}$), c is the concentration of MTSEA (M), and t is the incubation time (300 s).

Molecular Models of the μ Opioid Receptor. The model of the MOPR was constructed by homology modeling techniques using the crystal structure of bovine rhodopsin (PDB code 1GZM) (18) as template, in a similar manner to the previously reported model of the δ opioid receptor (16), and using the very recent crystal structures of the β_2-adrenergic receptor (PDB codes 2RH1 and 2R4R) (6−8) and the ligand-free opsin (PDB code 3CAP) (9) as template. The structure of the inactive conformation of the homodimer was modeled, from the rhodopsin-based model, in such a manner that substituted cysteines at positions 4.41, 4.44, 4.48, 4.51, and 4.59 could be cross-linked, as suggested by Guo et al. (19). In contrast, the pattern of cross-linking in the active conformation of the receptor is at positions 4.50, 4.54, and 4.58, which requires either a rotation of TM4, displacement of protomers, or protomer exchange (19). Rotation of TM4 was performed in steps of 5° along its axis, in a counter-clockwise path, viewed from the extracellular side, until the proposed disulfide bridges between the substituted cysteines were formed. The model corresponding to displacement of protomers was obtained by interactive computer graphics until formation of disulfide bridges. Finally, the proposed model of the rhodopsin oligomer (PDB code 1N3M) (20) was employed as a starting point to study the mechanism of protomer exchange. These models were refined by molecular dynamics (MD) simulations. A positional restraint of 1 kcal mol^{-1} Å^{-2} was applied to the C_α atoms of a fixed monomer, while the torsion angles ϕ and ψ of the moving monomer were maintained close to the initial conformation with flat harmonic restraints of 32 kcal mol^{-1} Å^{-2}. This procedure permits one monomer to move relative to the other to form the proposed disulfide bridges between protomers without

modifying the initial TM bundle of the receptor. These models resemble the recently proposed structures of 7TMR oligomerization (21). The MD simulations were performed with the Sander module of AMBER 9 (22), a 2 fs integration time step, constant temperature of 300 K, and the Duan et al. force field.

Nomenclature of the Side Chain Conformation. The side chain conformation has been categorized into *gauche*$^-$ (0° < χ < 120°), *trans* (120° < χ < 240°), or *gauche*$^+$ (240° < χ < 360°) depending on the value of the torsional χ angle.

Data Analysis. Data were analyzed by one-way analysis of variance (ANOVA) followed by the post hoc Dunnett multiple comparison test using $P < 0.05$ as the level of significance.

RESULTS

K_d and B_{max} Values of the Antagonist [3H]Diprenorphine for the WT and Mutants of the μ Opioid Receptors Transiently Expressed in HEK293 Cells. The WT and mutant receptors were transiently transfected into HEK293 cells. Saturation binding of [3H]diprenorphine to the receptors was performed on intact cells, and K_d and B_{max} values were determined (Table 1). The single mutants C7.38(321)S, D3.49(164)Y, and T6.34(279)K had similar affinities for [3H]diprenorphine as the WT receptor. The double mutants D3.49Y/C7.38S and T6.34K/C7.38S also exhibited similar K_d values for [3H]diprenorphine compared with the D3.49(164)Y background.

The triple mutants bound [3H]diprenorphine with similar K_d values as the D3.49(164)Y/C7.38(321)S background, with the exception of C6.47(292)S/D3.49(164)Y/C7.38(321)S, which displayed a significant loss in the affinity for [3H]diprenorphine. Thus, mutations to serines of the cysteine residues in TMs, except C6.42, on the background of D3.49(164)Y/C7.38(321)S did not overly affect the overall structure of the receptor compared to the background.

Effects of Mutations on Affinity for the Agonist DAMGO. One important characteristic of many CAM receptors is increased affinities for agonists and decreased affinities for inverse agonists (23). We previously demonstrated that the

Table 2: Second-Order Rate Constants of Reaction of MTSEA (M^{-1} s^{-1}) with Wild Type and Mutants of the Rat MOPRs Transiently Expressed in HEK Cells[a]

construct	second-order rate constant (M^{-1} s^{-1})
RMOPR WT	$3.7 \pm 0.56(3)$
C7.38(321)S	$0.42 \pm 0.08(4)$[b]
D3.49(164)Y	$4.3 \pm 0.34(4)$
D3.49(164)Y/C7.38(321)S	$4.4 \pm 0.38(3)$
C1.49(79)S/D3.49Y/C7.38S	$5.5 \pm 1.28(3)$
C3.44(159)S/D3.49Y/C7.38S	$1.3 \pm 0.45(4)$[b]
C4.48(190)S/D3.49Y/C7.38S	$1.6 \pm 0.26(3)$[b]
C5.41(235)S/D3.49Y/C7.38S	$2.5 \pm 0.65(6)$[c]
C5.57(251)S/D3.49Y/C7.38S	$6.1 \pm 0.59(4)$
C6.47(292)S/D3.49Y/C7.38S	no binding detected
C7.47(330)S/D3.49Y/C7.38S	$1.9 \pm 0.50(5)$[b]

[a] Cells were treated with at least four concentrations of MTSEA, and [³H]diprenorphine binding was performed on washed cells. In most cases, 0.1, 0.25, 1, and 2.5 mM MTSEA were used. The second-order rate constant for each construct was calculated as described under Materials and Methods. Data represent the mean $\pm$ SEM of three to seven independent experiments in duplicate. [b] $P < 0.01$, compared with D3.49(164)Y/C7.38(321)S by one-way ANOVA followed by the post hoc Dunnett multiple comparison test. [c] $P < 0.05$.

constitutively active mutant D3.49(164)Y had higher affinities for the agonist DAMGO that were 20-fold that of the WT in membrane binding (*10, 11*). The affinities of DAMGO to the WT and mutants were determined in intact cells by competitive inhibition of [³H]diprenorphine binding to the receptor (Table 1). The apparent K_i of DAMGO for the WT was determined to be 432 ± 80 nM in intact cells, which was much greater than the K_i value determined in membrane (3−6 nM) (*10, 11*). This is in agreement with the previous reports that Na$^+$ in binding buffer reduced the receptor affinity for agonists and DAMGO exhibited much lower affinities for the MOPR in intact cells than in membrane (*24*). The double mutant D3.49(164)Y/C7.38(321)S had similarly high affinities for DAMGO as the D3.49(164)Y background, and the two mutants exhibited higher affinities for DAMGO than the WT. These results indicate that D3.49(164)Y/C7.38(321)S retains high agonist affinity of the constitutively active mutant D3.49Y. As shown in Table 1, the triple mutants displayed similar or even higher affinities for DAMGO than the background D3.49(164)Y/C7.38(321)S, which represented 4−24-fold increases in their affinities for DAMGO compared with the WT, indicating that these triple mutants still exhibit constitutively active mutant (CAM) phenotypes. Interestingly, the T6.34(279)K mutant exhibited higher affinity for DAMGO than the D3.49(164)Y mutant, and the T6.34K/C7.38S mutant had similar affinity as the T6.34(279)K mutant.

Effects of MTSEA Pretreatment on [³H]Diprenorphine Binding to the WT and Mutants. To identify the cysteine(s) within the TMs of the D3.49(164)Y mutant that became accessible in the binding pocket, we quantitated the reaction of the −SH groups of accessible or inaccessible cysteines of the TMs of the D3.49(164)Y mutant with MTSEA by comparing the second-order rate constants.

As shown in Table 2, the D3.49(164)Y mutant had similar sensitivity to MTSEA as the WT. We have demonstrated that among the eight cysteines in the TMs of the WT, C7.38(321) was solely accessible in the binding pocket and conferred the sensitivity of the WT to MTSEA (*14*). The double mutant D3.49(164)Y/C7.38(321)S had similar MT-SEA sensitivity as D3.49(164)Y, indicating that C7.38(321)

either becomes inaccessible or other cysteines become exposed and contribute to the MTSEA sensitivity.

The triple mutants generated on the background of the double mutant D3.49(164)Y/C7.38(321)S showed different sensitivities to MTSEA. The second-order rate constants of reaction with MTSEA showed that the C3.44(159)S, C4.48(190)S, C5.41(235)S, and C7.47(330)S mutants on the D3.49(164)Y/C7.38(321)S background were significantly less sensitive to MTSEA than D3.49(164)Y/C7.38(321)S, but C1.49(79)S and C5.57(251)S mutants were not. It is noteworthy that of the two cysteines in the TM5, C5.41(235) at the extracellular side of the TM5 of the D3.49(164)Y CAM became accessible to the binding pocket; however, C5.57(251) at the cytoplasmic side of the TM5 did not. Taken together, we hypothesize that C3.44(159), C4.48(190), C5.41(235), and C7.47(330) of the D3.49Y may be rotated and/or tilted to become accessible in the binding pocket.

That four cysteine residues contribute in part to MTSEA sensitivity of the D3.49Y/C7.38S mutant suggests that mutations of all four Cys residues should render the receptor insensitive to MTSEA. We have generated a mutant on the D3.49Y/C7.38S background containing these four Cys to Ser mutations. However, this mutant did not exhibit any [³H]diprenorphine binding, thus precluding assessment of its MTSEA sensitivity.

Comparison between the D3.49(164)Y and T6.34(279)K Mutants. We have shown that mutation of Thr6.34(279) to Lys in the C-terminal portion of the third intracellular loop leads to constitutive activation of the receptor (*11*). The T6.34(279)K mutant exhibited binding affinity for [³H]diprenorphine similar to the wild type, with a K_d value of 0.17 ± 0.02 nM, and a much higher affinity for DAMGO than the wild type, with a K_i value of 6.3 ± 1.1 nM ($n = 3$). MTSEA (2.5 mM) treatment inhibited [³H]diprenorphine binding to the T6.34(279)K mutant more than that to the wild type or the D3.49(164)Y mutant. The T6.34(279)K/C7.38(321)S mutant retains the binding property of the T6.34K mutant with a K_d value of 0.24 ± 0.01 nM for [³H]diprenorphine and a K_i value of 10 ± 1 nM for DAMGO ($n = 3$). While the T6.34(279)K/C7.38(321)S mutant displayed much lower sensitivity to MTSEA than the T6.34(279)K mutant, the D3.49(164)Y/C7.38S mutant was not significantly different from the D3.49 mutant (Figure 2). These results suggest that the two constitutively active mutants may assume different conformations and/or possess different dynamic properties and flexibility.

Molecular Models of the MOPR Monomer and Homodimer. In order to analyze in a structural context the putative movements of TMs 3, 4, 5, and 7 upon constitutive agonist-independent receptor activation, we constructed a molecular model of the MOPR (see Materials and Methods). Figure 1B shows the positions of the eight cysteines in the TM domain of the receptor. Besides, there is significant evidence that 7TMRs can form either homodimers or heterodimers (see ref *25* for a review), including opioid receptors (*26*). Guo et al. (*19*) have mapped the dimer interface in the dopamine D2 receptor over the entire length of TM4 by cross-linking of substituted cysteines. They found that inverse agonists, favoring the inactive conformation of the receptor, cross-link at positions 4.41, 4.44, 4.48, 4.51, and 4.59. Interestingly, these positions appear to be conserved hydrophobic residues in the rhodopsin-like family of 7TMRs
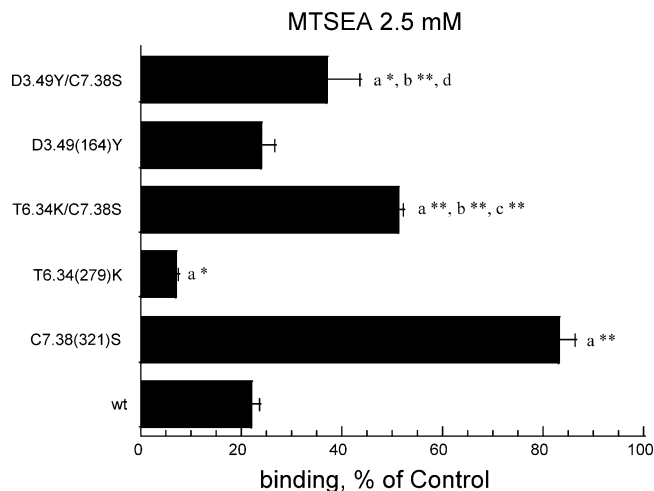
FIGURE 2: Effect of MTSEA pretreatment on [³H]diprenorphine binding to the wild type and mutants of the rat MOPR. HEK293 cells transiently transfected with the wild type or a mutant of the rat MOPR were treated with 2.5 mM MTSEA or vehicle (as control) for 5 min at room temperature. [³H]Diprenorphine binding was performed on intact cells after washing as described in Materials and Methods. Each point represents the mean ± SEM of three independent experiments in duplicate. Data were analyzed by one-way ANOVA followed by the post hoc Dunnett multiple comparison test. *, $P < 0.05$. **, $P < 0.01$. a, significantly different from wt. b, significantly different from C7.38(321)S. c, significantly different from T6.34(279)K. d, not significantly different from D3.49(164)Y. Other comparisons not listed.

Table 3: Amino Acids at Positions 4.41, 4.44, 4.48, 4.51, and 4.59 in TM4 of the Dopamine D2 Receptor, μ Opioid Receptor, and Class A 7TMRs

	position				
	4.41	4.44	4.48	4.51	4.59
dopamine D2	Arg	Val	Ile	Val	Pro
μ opioid	Asn	Ile	Cys	Ile	Pro
class A 7TMRs	Arg 25%	Ala 13%	Ala 20%	Ala 20%	Ile 13%
	Lys 8%	Leu 23%	Leu 20%	Leu 24%	Gly 7%
	His 8%	Val 17%	Val 13%	Val 25%	Met 2%
	Asn 4%	Ile 11%	Ile 8%	Met 2%	Leu 15%
	Gln 4%	Gly 6%	Gly 16%	Cys 5%	Pro 65%
total	49%	76%	84%	91%	80%

with the exception of position 4.41 (Table 3). Dopamine D2 receptor, μ opioid receptor, and class A 7TMRs contain Val, Ile, and hydrophobic amino acids in 76% of the sequences, respectively, at position 4.44; Ile, Cys, and hydrophobic in 84% of the sequences at position 4.48; Val, Ile, and hydrophobic in 91% of the sequences at position 4.51; and Pro and hydrophobic in 80% of the sequences at position 4.59 (27). Position 4.41 is mostly polar, being Arg in the D2 receptor and Asn in the μ opioid receptor. This conservation pattern among the D2 receptor, the μ opioid receptor, and other 7TMRs suggests a common dimer interface. Figure 3 shows the molecular model of the MOPR homodimer in which the proposed disulfide bridges between the substituted cysteines at these positions are formed. The initial structure of the monomer (in gray ribbons) are superimposed to each protomer of the dimer to illustrate that the proposed interface can be achieved without modifying the initial TM bundle of the receptor.

DISCUSSION

The D3.49(164)Y and T6.34(279)K Mutants Appear To Represent Different Activated States. The interaction between
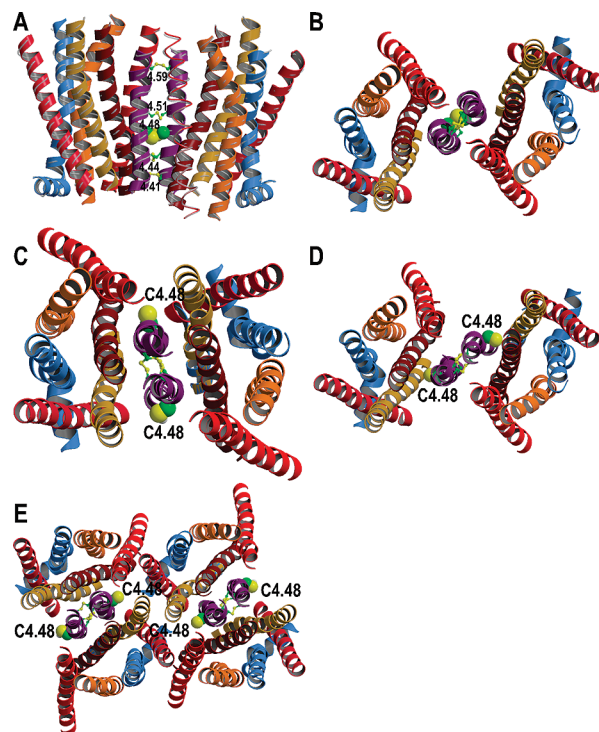

FIGURE 3: Molecular model of the MOPR homodimer. C4.48(190) is shown as van der Waals spheres. The dimer interface of the inactive conformation (panels A and B) and the proposed active conformation of transmembrane helix 4 (panels C−E) are modeled as suggested by Guo et al. (*19*). In the presence of inverse agonists, favoring the inactive conformation, the receptors cross-link substituted cysteines at positions 4.41, 4.44, 4.48, 4.51, and 4.59 (panels A and B). In contrast, agonists, favoring the active conformation of the receptor, cause cross-linking at positions 4.50, 4.54, and 4.58 (panels C−E), which requires either a displacement of protomers (panel C), rotation of TM4 (panel D), or protomer exchange (panel E). The color code of the helices is as in Figure 1B.

R3.50 of the highly conserved (D/E)R(Y/W) motif in TM3 with its adjacent D/E3.49 and D/E6.30 near the cytoplasmic end of TM6 in rhodopsin is known as the ionic lock (*28*). In the inactive structure of rhodopsin, R3.50 in TM3 interacts with E6.30 (the interatomic distance between C$_\alpha$ atoms is 8.7 Å and between heteroatoms is 2.9 Å) and T6.34 (6.7 Å and 3.6 Å) in TM6 (*4*). While the (D/E)R(Y/W) motif in TM3 is highly conserved in class A 7TMRs, the acidic residue at position 6.30 is only present in 32% of the sequences (D, 7%; E, 25%) (*27*). Opioid receptors feature L6.30(275) and T6.34(279) in TM6, so R3.50(165) interacts with D3.49(164) and with T6.34(279) (*11, 29*) (Figure 4A).

We have previously shown that the D3.49(164)Y and T6.34(279)K mutants display different levels of constitutive activities (*10, 11*). We found here that the C7.38(321)S/D3.49(164)Y mutant was similarly sensitive to MTSEA as the D3.49(164)Y mutant, while the C7.38(321)S/T6.34(279)K mutant showed greatly reduced sensitivity to MTSEA compared with the T6.34(279)K mutant. These results confirm that the two constitutively active mutants D3.49(164)Y and T6.34(279)K may assume different conformations. The T6.34(279)K mutation makes the interaction with R3.50(165) in TM3 incompatible. Thus, the absence of this interaction probably induces the intracellular part of TM6 to move outward as observed in the crystal structure of the ligand-free opsin (*9*). Figure 4B shows the proposed conformation of TM6 in opaque orange [the position of TM6 depicted in
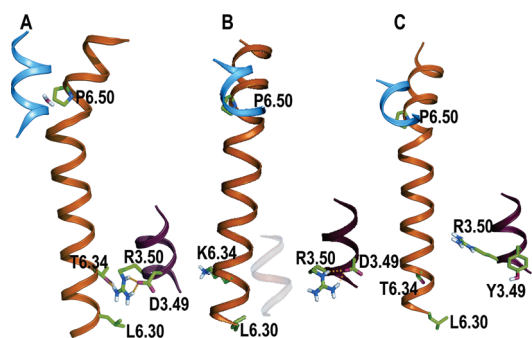
FIGURE 4: Detailed view of the network of interactions within TMs 3 (darkred), 6 (orange), and 7 (blue) of the MOPR. (A) The strong distortion of TM6 at P6.50 is partly stabilized, in addition to a discrete water molecule located in the vicinity of P6.50 (*49*), by the ionic interaction between R3.50 in TM3 with T6.34 near the cytoplasmic end of TM6 in the rhodopsin-based model of the *μ* opioid receptor. (B) The T6.34K mutant receptor introduces an electrostatic repulsion with the also positively charged R3.50, relocating TM6. TM6 is modeled based on the structure of ligand-free opsin. The position of TM6 in wild-type MOPR is shown in transparent orange for comparison purposes. (C) The D3.49Y mutant disrupts the ionic interaction with R3.50, allowing its side chain to shift out from the polar pocket, to point toward the protein core. The opsin-based model of the MOPR is shown.

Figure 4A, interacting with R3.50(165), is also shown in transparent orange for comparison purposes], modeled based on the structure of opsin (see Materials and Methods). The conformation of the T6.34(279)K mutant receptor probably resembles 34% of class A 7TMRs containing a basic residue at position 6.30 (K, 18%; R, 16%). R6.30D and R6.30E substitutions in the chemokine CCR5 receptor, which allow an ionic interaction with R3.50, resulted in a receptor devoid of constitutive activity (*30*). The D3.49(164)Y mutant disrupts the ionic interaction with the nearby R3.50(165), allowing the side chain of R3.50(165) to shift out from the polar pocket (Figure 4C for the opsin-based receptor model). The structure of the ligand-free opsin has confirmed the previous proposal by Bakker et al. (*31*) for the histamine H_1 receptor that R3.50 performs a conformational change from the inactive χ_1:*trans*, χ_2:*gauche⁻*, χ_3:*gauche⁺*, χ_4:*gauche⁻* conformation, engaged in the ionic lock (Figure 4A), to the active χ_1:*gauche⁺*, χ_2:*trans*, χ_3:*trans*, χ_4:*trans* conformation, pointing toward the protein core (Figure 4C). This has two effects on the structure of the receptor. First, it disrupts the interaction between TMs 3 and 6, permitting the movement of the cytoplasmic end of TM6 away from TM3 in a similar manner to the T6.34(279)K mutant (Figure 4B). Second, it allows the polar side chain of R3.50(165) to interact with other amino acids of the receptor. It is important to note that disruption of the ionic lock has a large energetic cost that must be compensated by the formation of new stabilizing interactions in the resulting active state of the receptor. We have proposed that R3.50(165) can form a direct or indirect, through other side chains and/or internal water molecules, interaction with the acidic D2.50(114)···N7.49(332) pair in the active state of the receptor (*31, 32*). Thus, we hypothesize that the T6.34(279)K mutant receptor triggers the movement of TM6 away from TM3 at the intracellular side (Figure 4B), while the D3.49(164)Y mutant triggers, in addition to this movement of TM6, the conformational transition of R3.50(165) (Figure 4C).

Studies support multiple activated states of 7TMRs (see ref *33* for a review). For instance, in the α_{1B}-AR, mutation

of A6.34(293) in the C-terminal region of the third intra-cellular loop to all 19 possible amino acids resulted in different degrees of constitutive activities (*34*). We have shown that mutation of D3.49(164) to H, Q, Y, and M in the MOPR led to different levels of constitutive activities (*10*). Two different constitutively active mutants of the α_{1B}-AR, the A6.34(293)E and the D3.49(142)A mutants, are differentially phosphorylated and internalized although they have similar agonist-independent activities (*35*). Fluorescence spectroscopy analysis of the purified β_2-adrenergic receptor gave more direct structural evidence that ligands cause alterations in receptor structure in agreement with the existence of multiple conformational states (*36*).

Movements of TMs Involved in Activation of the μ Opioid Receptor. There are eight cysteines of the TMs of the rat MOPR (Figure 1), and C7.38(321) is solely accessible in the binding-site crevice of the wild-type receptor as inferred by the effect of MTSEA on [³H]diprenorphine binding (*14*). Among the remaining seven cysteines, we found that C3.44(159)S, C4.48(190)S, C5.41(235)S, or C7.47(330)S mutation partially reduced the sensitivity of the D3.49(164)Y/ C7.38(321)S mutant to MTSEA, indicating that these four Cys residues become accessible in the binding-site crevice. These results suggest these Cys residues are tilted or rotated, and movements of TMs 3, 4, 5, and 7 are associated with constitutive activation of the rat *μ* opioid receptor. Farrens et al. (*37*) showed that activation of rhodopsin involved rigid-body movement of several TMs. For other 7TMRs, specific movements of single or two TMs are shown to be related to activation (see reviews in refs *5−8* and references cited therein). The recent crystal structure of the ligand-free opsin (*9*) contains, compared to rhodopsin, structural changes characteristic of an active 7TMR state. Among them, the intracellular part of TM6 is tilted outward by 6−7 Å, and TM5 is close to TM6. This new structure, thus, opens an opportunity to model several key features of the process of 7TMR activation. Therefore, the putative changes in con-formations of TMs 3, 4, 5, and 7 were analyzed in molecular terms using constructed models of the *μ* opioid, based on the inactive structures of rhodopsin and the β_2-adrenergic receptor, and the partially active structure of opsin, together with experimental results.

TM3. Our results show that the C3.44(159)S/D3.49(164)Y/ C7.38(321)S mutant of the *μ* opioid receptor, which retains the CAM phenotype, is less sensitive to MTSEA than the background D3.49(164)Y/C7.38(321)S, indicating that C3.44(159) becomes exposed in the binding-site crevice. Since C3.44(159) was not accessible in wild-type MOPR (*14*), we suggest that movement of C3.44(159) occurs in the constitutive active D3.49(164)Y mutant. This is in agreement with previous findings by Gether et al. (*38*), who reported that agonist activation of the β_2-AR caused C3.44(159) and C6.47(285) to be exposed to a more polar environment, indicating that conformational changes occur around these two residues. Figure 5A shows the orientation of C3.44(159), toward TM5, in the rhodopsin-based model of the inactive conformation of the *μ* opioid receptor. Panels B and C of Figure 5 show the opsin-based model of the MOPR superimposed onto the inactive model of the receptor (in tube ribbons). The D3.49(164)Y mutation allows R3.50(165) to adopt the extended conformation, pointing toward the protein core, permitting the movement of TM6 toward TM5 and its
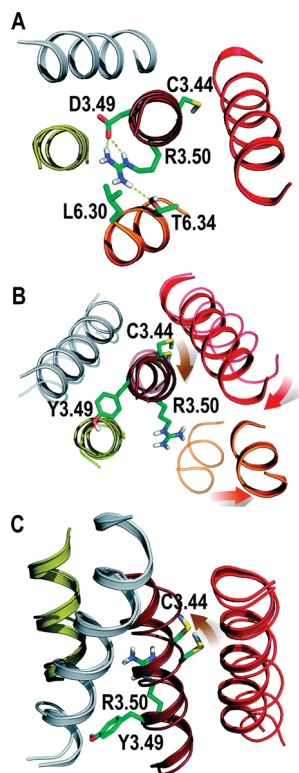
FIGURE 5: Detailed view of TMs 2 (goldenrod), 3 (darkred), 4 (gray), 5 (red), 6 (orange), and 7 (blue) in the rhodopsin-based (A) and opsin-based (B, C) models of the μ opioid receptor. (A) Orientation of C3.44(159) toward TM5 in the rhodopsin-based model of the inactive conformation of the receptor. (B, C) Opsin-based model of the MOPR superimposed to the rhodopsin-based model (in tube ribbons). Structures in panel B are rotated 90° to become those in panel C. While TMs 2 and 4 remain unchanged in both structures, TMs 3, 5, and 6 perform significant movements, making C3.44(159) point toward the binding-site crevice.

subsequent relocation (see arrows in Figure 5B). Clearly, while TMs 2 and 4 remain unchanged in both structures, TM3 also performs a significant movement (see arrow in Figure 5B,C). This includes a clockwise rotation, viewed from the intracellular side (Figure 5C), which orients C3.44(159) toward the binding-site crevice, in agreement with previous observations (*38*).

TM4. The C4.48(190)S/D3.49(164)Y/C7.38(321)S mutant, which displays high affinity for DAMGO similar to the D3.49(164)Y mutant, had lower sensitivity to MTSEA than the D3.49Y(164)/C7.38(321)S background. This result indicates that C4.48(190) in the middle of TM4 contributes in part to the MTSEA sensitivity. Since C4.48(190) appears inaccessible in the binding pocket of the wild-type μ opioid receptor, we suggest that C4.48(190) is turned or tilted to become exposed. Notably, the crystal structure of the ligand-free opsin does not show any significant movement of TM4 (*9*).

A three-dimensional structure of squid rhodopsin determined by cryoelectron microscopy of two-dimensional crystals features a symmetric interface of the homodimer involving TM4 (*39*). In addition, the dopamine D2 receptor can be oxidatively cross-linked at positions 4.41, 4.44, 4.48, 4.51, and 4.59 (*19*). These experimental results and the conservation pattern at the dopamine D2 receptor, μ opioid receptor, and class A 7TMRs (see Results) point to TM4 as a key domain involved in the dimer interface. In particular, C4.48(190) of the MOPR homodimer in the inactive state

(Figure 3A,B) is located at the dimer interface and, thus, is inaccessible from the binding-site crevice. In contrast, Guo et al. (*19*) have also shown that in the presence of agonists, favoring the active conformation, the D2 receptors cross-link at positions 4.50, 4.54, and 4.58, which requires either a displacement of protomers, rotation of TM4, or protomer exchange. Figure 3C shows the result of displacing monomer B, relative to monomer A, of the MOPR to form the proposed disulfide bridges between protomers at the active state of the receptor (see Materials and Methods). Clearly, C4.48(190) is exposed to the lipidic environment and, in disagreement with the experimental results, is inaccessible from the binding-site crevice. TM4 was also rotated in steps of 5° along its axis, in a counterclockwise path, viewed from the extracellular side, until the proposed disulfide bridges between the substituted cysteines at positions 4.50, 4.54, and 4.58 were formed. Figure 3D shows the final model in which TM4 was rotated 120°. C4.48(190), in this model, is pointing between TMs 2 and 3 and, in agreement with the experimental results, is exposed to the binding-site crevice. Finally, Figure 3E shows the mechanism in which protomers change partners (see Materials and Methods). C4.48(190) is not exposed to the binding-site crevice in the protomer exchange mechanism. It has been suggested by theoretical calculations that the rotation of TM4s along the helical axes is an unlikely mechanism, whereas protomer displacement and protomer exchange result to be equally feasible dynamic motions (*21*). However, our results can only be explained by the notion that rotation of TM4 makes C4.48(190) to point toward the binding-site crevice, in contrast to the other proposed mechanisms (*19*).

TM5. The C5.41(235)S/D3.49Y/C7.38S mutant displays similar affinity for DAMGO as the D3.49(164)Y mutant, indicating that this mutant represents an activated form of the receptor. This mutant is less sensitive to MTSEA than the D3.49(164)Y/C7.38(321)S background, indicating that C5.41(235) becomes accessible in the binding-site crevice. We previously showed that C5.41(235) at the extracellular side of TM5 of the rat μ WT was inaccessible in the binding pocket (*14*), in agreement with findings that S5.41(199) of the human α$_{2A}$-AR faces the lipid bilayer (*40*). Our result that C5.41 of the D3.49Y mutant became accessible in the binding pocket suggests that movement of TM5 is associated with receptor activation, in accord with the finding that agonist binding induces rotation of TM5 in the human α$_{2A}$-AR (*41*). Using the substituted cysteine accessibility method and two sulfhydryl reagents, Marjamaki et al. (*41*) found that in the α$_{2A}$-AR the rate of reaction of the agonist chloroethylclonidine with C5.42(200) was more than 5 times that of MTSEA, while reaction rates were similar for substituted Cys residues at 5.39(197), 5.43(201), and 5.46(204). Their results suggest that C5.42(200) may be induced by chloroethylclonidine to turn and react with the compound, and rotation of C5.42(200) may be associated with receptor activation.

Panels A and B of Figure 6 show the position of C5.41(235) and C5.57(251) in the rhodopsin-based molecular model of the μ opioid receptor. In this model C5.41(235) and C5.57(251) are located at the same face of the helix, pointing toward the lipidic environment, and thus far from the binding-site crevice. Panels C and D of Figure 6 show the opsin-based model of the MOPR superimposed to the inactive model of the receptor (in tube ribbons). As revealed
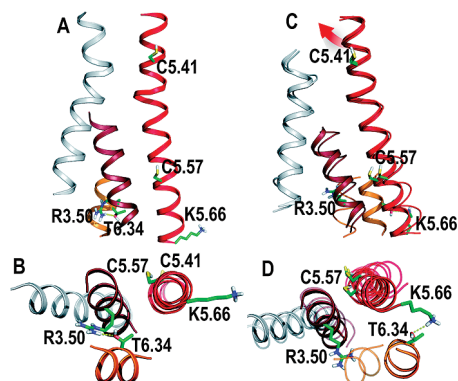
FIGURE 6: (A, B) Orientation of C5.41(235) and C5.57(251) in TM5 (red) in the rhodopsin-based molecular model of the μ opioid receptor. (C, D) The opsin-based model of the MOPR superimposed to the inactive model of the receptor (in tube ribbons). Structures in panels A and C are rotated 90° to become panels B and D.

FIGURE 7: (A) Orientation of C7.47(330) in TM7 (blue) toward TM1 (crimson) in the inactive conformation of the β_2-AR based molecular model of the μ opioid receptor. TM7 contains a highly distorted and probably functional P7.50 kink, which is stabilized by the hydrogen bond interaction between N1.50 and the 7.46 carbonyl oxygen, a water molecule linking the 1.47 and 7.47 carbonyl oxygens, and a second water molecule located between the carbonyl at position 7.45 and the N−H amide at position 7.49. (B) Superimposition of the opsin-based and the β_2-based (in tube ribbons) molecular models of the receptor. TM7 performs a conformational reorganization in the region of P7.50(333).

in the original publication of opsin (*9*), the movement of TM6 toward TM5 facilitates the interaction between T6.34(279) and K5.66(260) for stabilizing the active conformation of the receptor (Figure 6D). In order to achieve this key interaction, TM5 has also to move toward the protein core and perform a clockwise rotation, viewed from the intracellular side (Figure 6D). This rotation of TM5 further removes C5.57(251) from the binding-site crevice. Importantly, while C5.57(251) at the intracellular side of TM5 remains inaccessible in the constitutively active mutant receptor, C5.41(235) at the extracellular side becomes accessible to the binding pocket. Nevertheless, the structure of opsin does not show any difference at the extracellular part of TM5 relative to inactive rhodopsin (Figure 6C). The fact that the crystal structure of opsin does not contain agonist-inducing receptor activation in the binding site suggests that, in contrast to the intracellular domain of the receptor, the extracellular part has not accomplished the key features of the active state. For instance, W6.48 of the CWxP(F/Y) motif (*42, 43*) or N7.49 of the NPxxY motif (*31, 32*) has not modified their rotamer side chain conformation as has been suggested. In addition, fluorescence spectroscopy, monitoring agonist-induced conformational changes of the β_2-adrenergic receptor, has shown that agonist binding induces the conformational transition of the extracellular part of TM5 toward the binding-site crevice stabilized by the interactions between Ser residues in TM5 and the catechol hydroxyls of the ligand (*44*). In agreement with these results, our data suggest that receptor activation would induce the movement (arrow in Figure 6C) of the extracellular domain of TM5 toward the bundle, making C5.41(235) accessible to the binding pocket.

TM7. There are two cysteines, C7.38(321) and C7.47(330), in TM7 of the rat μ opioid receptor, which are close to the highly conserved N(7.49)P(7.50)XXY(7.53) motif, a critical region for signaling and agonist-induced internalization of several 7TMRs. C7.38(321) was previously found to be accessible in the binding-site crevice of the wild-type μ receptor. C7.38(321)S mutation in the D3.49Y mutant did not change the sensitivity of the mutant to MTSEA, indicating that C7.38(321) is inaccessible in the binding-site crevice and there are other cysteine residues being exposed. The D3.49(164)Y/C7.38(321)S/C7.47(330)S mutant, having a similar affinity for DAMGO as the D3.49Y
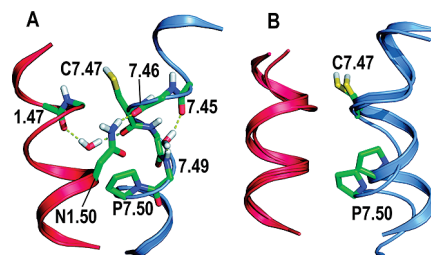
mutant, displayed lower MTSEA sensitivity than the D3.49Y/ C7.38(321)S mutant, indicating that C7.47 is turned to be accessible in the binding-site crevice. These results suggest that TM7 movement is associated with receptor activation, which are consistent with the findings on rhodopsin, β_2-adrenergic receptor, and complement factor 5a receptor (C5aR). F6.44(282)L mutation of the β_2-AR, which resulted in constitutive activation of the receptor, induces movement of Cys 7.54(327) in TM7, in addition to Cys6.47(285) in TM6 (*45*). Using site-directed monoclonal antibodies, Abdulaev et al. (*46*) showed that light induces the exposure of 7.51(304)−7.58(311) residues of TM7, which correlates with formation of the metarhodopsin II, indicating that the movement of TM7 is important for rhodopsin activation. In the β_2-AR, D3.32(113)H/N7.39(312)H substitutions created a metal ion binding site, and binding of Zn^{2+} or Cu^{2+} activated the receptor, indicating the involvement of TM7 movements in receptor activation (*47*). Baranski et al. (*48*) reported that a mutant of the C5a receptor with TM7 truncated displayed constitutive activities, suggesting that TM7 may act as the ligand-sensing inhibitor of receptor activation, and movements of TM7 relieve constraints that hold the receptor in the inactive state.

Figure 7A shows the environment of P7.50 in the β_2-based molecular model of the μ opioid receptor and the orientation of C7.47(330) toward TM1. We have chosen the β_2-based molecular model to analyze the TM1−TM7 interface because both opioid and β_2-adrenergic receptors feature the GN(1.50) motif in TM1, in contrast to rhodopsin that contains the PxN(1.50) motif. The class A family of 7TMRs contains the highly conserved P7.50, present in 96% of the sequences (*27*). However, the conformation of this helix is far from being a standard Pro-kinked helix. This highly distorted and probably functional P7.50 kink is stabilized by the hydrogen bond interaction between the highly conserved N1.50 (100% of the sequences) in TM1 and the 7.47 carbonyl oxygen, a water molecule linking the 1.47 and 7.47 carbonyl oxygens (which is first reported in the crystal structure of the β_2-adrenergic receptor) and a second water molecule located between the carbonyl at position 7.45 and the N−H amide at position 7.49 (Figure 7A) (*49*). As a result the intrahelical hydrogen bond distance between N_i and O_{i-4}, which in standard α-helices is about 3.0 Å, amounts to 4.9 Å in the receptor model (this distance is 2.8 Å in the opsin-based

model; see below). It has been shown for rhodopsin that mutant P7.50A forms normal Meta II and shows hyperactivity after illumination (*50*). It was hypothesized that receptor activation leads to reorganization of this region of TM7, which is favored by Ala at position 7.50, probably by its propensity to form an α-helix (*50*). Figure 7B shows the superimposition of the opsin-based and the β_2-based (in tube ribbons) molecular models of the receptor. Clearly, TM7 performs a conformational reorganization in the region of P7.50(333), which resembles a more standard helical conformation. Nevertheless, this new conformation of TM7 keeps the orientation of C7.47(330) toward TM1 and far from the binding-site crevice.

Potential Limitation of Mutagenesis and Computational Studies. Alterations resulting from the mutation can be due to changes in the locus mutated, global conformational changes in the receptor, and local conformation changes in or around the binding pocket. If there are changes in the affinity of the mutant to ligands, it suggests that the binding pocket has been altered and the mutant cannot be used to assess changes in accessibility in the binding-site crevice. When any mutation greatly reduces or even abolishes receptor expression, such as the case of the C6.47(292)S/D3.49(164)Y/C7.38(321)S mutant, no assessment can be made regarding whether there is a change in accessibility. In addition, based on the results that C3.44(159)S, C4.48(190)S, C5.41(235)S, and C7.47(330)S mutants on the D3.49(164)Y/C7.38(321)S background were significantly less sensitive to MTSEA, we generated a mutant containing six mutations, C3.44(159)S/C4.48(190)S/C5.41(235)S/C7.47(330)S/D3.49(164)Y/C7.38(321)S. Unfortunately, this mutant did not exhibit any detectable [^{3}H]diprenorphine binding, preventing further MTSEA sensitivity studies.

The presence of cysteine residues in almost every TM in the MOPR presented an advantage and a challenge for this study. The advantage is that we can utilize the cysteine residues as a sensor for the movement of TMs. The results that C3.44(159)S, C4.48(190)S, C5.41(235)S, and C7.47(330)S mutations on the D3.49(164)Y/C7.38(321)S background reduced the sensitivity to MTSEA suggest that these four Cys residues may be exposed to the binding-site crevice in the constitutively active mutant. This interpretation is based on the assumption that Cys-to-Ser mutations do not affect the receptor structure other than the locus mutated. Since Ser has similar size and charge as Cys, the assumption should be valid in most cases. However, one cannot rule out the possibility that mutation of one cysteine may cause changes in the receptor structure, due to disruption of a disulfide bond or changes in the local environment, thereby allowing one or more previously inaccessible cysteine residues to become exposed in the binding-site crevice. This scenario will greatly complicate interpretation of the study.

Future Studies. With the technical advancements in crystallography, high-resolution crystal structures of several 7TMRs have been solved, including rhodopsin, β_1- and β_2-adrenergic receptors, and ligand-free opsin (*4−9*). Christoffers et al. (*51*) have published a method to purify the wild-type MOPR epitope-tagged with FLAG at the N-terminus and c-myc and 6×His at the C-terminus by a combination of wheat germ agglutinin, nickel, and antibody affinity chromatography and gel filtration chromatography. We have previously demonstrated that β-funaltrexamine, an irreversible MOPR antagonist, binds covalently

to the MOPR (*52, 53*). β-Funaltrexamine-labeled MOPR is likely to represent inactive forms of the receptor, whereas unliganded MOPR may represent partially activated states. β-Funaltrexamine-bound MOPR epitope-tagged with FLAG at the N-terminus and c-myc and 6×His at the C-terminus may be purified similarly. Solving the crystal structures of ligand-free MOPR and β-funaltrexamine-bound MOPR may be an approach to delineate the changes occurring during receptor activation. Needless to say, these experiments are technically very challenging.

REFERENCES

1. Huang, P., and Liu-Chen, L.-Y. (2005) in *The G-Protein Coupled Receptors Handbook* (Devi, L. A., Ed.) pp 33−70, Humana Press Totowa, NJ.

2. Schwartz, T. W., Frimurer, T. M., Holst, B., Rosenkilde, M. M., and Elling, C. E. (2006) Molecular mechanism of 7TM receptor activation-a global toggle switch model. *Annu. Rev. Pharmacol. Toxicol 46*, 481–519.

3. Smit, M. J., Vischer, H. F., Bakker, R. A., Jongejan, A., Timmerman, H., Pardo, L., and Leurs, R. (2007) Pharmacogenomic and structural analysis of constitutive g protein-coupled receptor activity. *Annu. Rev. Pharmacol. Toxicol. 47*, 53–87.

4. Palczewski, K., Kumasaka, T., Hori, T., Behnke, C. A., Motoshima, H., Fox, B. A., Le Trong, I., Teller, D. C., Okada, T., Stenkamp, R. E., Yamamoto, M., and Miyano, M. (2000) Crystal structure of rhodopsin: A G protein-coupled receptor. *Science 289*, 739–745.

5. Warne, T., Serrano-Vega, M. J., Baker, J. G., Moukhametzianov, R., Edwards, P. C., Henderson, R., Leslie, A. G., Tate, C. G., and Schertler, G. F. (2008) Structure of a beta1-adrenergic G-protein-coupled receptor. *Nature 454*, 486–491.

6. Cherezov, V., Rosenbaum, D. M., Hanson, M. A., Rasmussen, S. G., Thian, F. S., Kobilka, T. S., Choi, H. J., Kuhn, P., Weis, W. I., Kobilka, B. K., and Stevens, R. C. (2007) High-resolution crystal structure of an engineered human beta2-adrenergic G protein-coupled receptor. *Science 318*, 1258–1265.

7. Rasmussen, S. G., Choi, H. J., Rosenbaum, D. M., Kobilka, T. S., Thian, F. S., Edwards, P. C., Burghammer, M., Ratnala, V. R., Sanishvili, R., Fischetti, R. F., Schertler, G. F., Weis, W. I., and Kobilka, B. K. (2007) Crystal structure of the human beta2 adrenergic G-protein-coupled receptor. *Nature 450*, 383–387.

8. Rosenbaum, D. M., Cherezov, V., Hanson, M. A., Rasmussen, S. G., Thian, F. S., Kobilka, T. S., Choi, H. J., Yao, X. J., Weis, W. I., Stevens, R. C., and Kobilka, B. K. (2007) GPCR engineering yields high-resolution structural insights into beta2-adrenergic receptor function. *Science 318*, 1266–1273.

9. Park, J. H., Scheerer, P., Hofmann, K. P., Choe, H. W., and Ernst, O. P. (2008) Crystal structure of the ligand-free G-protein-coupled receptor opsin. *Nature 454*, 183–187.

10. Li, J., Huang, P., Chen, C., de Riel, J. K., Weinstein, H., and Liu-Chen, L.-Y. (2001) Constitutive activation of the mu opioid receptor by mutation of D3.49(164), but not D3.32(147): D3.49(164) is critical for stabilization of the inactive form of the receptor and for its expression. *Biochemistry 40*, 12039–12050.

11. Huang, P., Li, J., Chen, C., Visiers, I., Weinstein, H., and Liu-Chen, L.-Y. (2001) Functional role of a conserved motif in TM6 of the rat mu opioid receptor: constitutively active and inactive receptors result from substitutions of Thr6.34(279) with Lys and Asp. *Biochemistry 40*, 13501–13509.

12. Akabas, M. H., Stauffer, D. A., Xu, M., and Karlin, A. (1992) Acetylcholine receptor channel structure probed in cysteine-substitution mutants. *Science 258*, 307–310.

13. Javitch, J. A., Shi, L., and Liapakis, G. (2002) Use of the substituted cysteine accessibility method to study the structure and function of G protein-coupled receptors. *Methods Enzymol. 343*, 137–156.

14. Xu, W., Chen, C., Huang, P., Li, J., de Riel, J. K., Javitch, J. A., and Liu-Chen, L.-Y. (2000) The conserved cysteine 7.38 residue is differentially accessible in the binding-site crevices of the mu, delta, and kappa opioid receptors. *Biochemistry 39*, 13904–13915.

15. Xu, W., Li, J., Chen, C., Huang, P., Weinstein, H., Javitch, J. A., Shi, L., de Riel, J. K., and Liu-Chen, L.-Y. (2001) Comparison of the amino acid residues in the sixth transmembrane domains accessible in the binding-site crevices of mu, delta, and kappa opioid receptors. *Biochemistry 40*, 8018–8029.

16. Xu, W., Campillo, M., Pardo, L., Kim, d. R., and Liu-Chen, L. Y. (2005) The seventh transmembrane domains of the delta and kappa opioid receptors have different accessibility patterns and interhelical interactions. *Biochemistry 44*, 16014–16025.

17. Ballesteros, J. A., and Weinstein, H. (1995) Integrated methods for the construction of three dimensional models and computational probing of structure-function relations in G-protein coupled receptors. *Methods Neurosci. 25*, 366–428.

18. Li, J., Edwards, P. C., Burghammer, M., Villa, C., and Schertler, G. F. (2004) Structure of bovine rhodopsin in a trigonal crystal form. *J. Mol. Biol. 343*, 1409–1438.

19. Guo, W., Shi, L., Filizola, M., Weinstein, H., and Javitch, J. A. (2005) Crosstalk in G protein-coupled receptors: changes at the transmembrane homodimer interface determine activation. *Proc. Natl. Acad. Sci. U.S.A. 102*, 17495–17500.

20. Liang, Y., Fotiadis, D., Filipek, S., Saperstein, D. A., Palczewski, K., and Engel, A. (2003) Organization of the G protein-coupled receptors rhodopsin and opsin in native membranes. *J. Biol. Chem. 278*, 21655–21662.

21. Niv, M. Y., and Filizola, M. (2008) Influence of oligomerization on the dynamics of G-protein coupled receptors as assessed by normal mode analysis. *Proteins 71*, 575–586.

22. Case, D. A., Darden, T. A., Cheatham, T. E., Simmerling, C. L., Wang, J., Duke, R. E., Luo, R., Merz, K. M., Pearlman, D. A., Crowley, M. et al. (2006) AMBER 9, University of California, San Francisco.

23. Hunyady, L., Vauquelin, G., and Vanderheyden, P. (2003) Agonist induction and conformational selection during activation of a G-protein-coupled receptor. *Trends Pharmacol. Sci. 24*, 81–86.

24. Toll, L. (1992) Comparison of mu opioid receptor binding on intact neuroblastoma cells with guinea pig brain and neuroblastoma cell membranes. *J. Pharmacol. Exp. Ther. 260*, 9–15.

25. Pin, J. P., Neubig, R., Bouvier, M., Devi, L., Filizola, M., Javitch, J. A., Lohse, M. J., Milligan, G., Palczewski, K., Parmentier, M., and Spedding, M. (2007) International Union of Basic and Clinical Pharmacology. LXVII. Recommendations for the recognition and nomenclature of G protein-coupled receptor heteromultimers. *Pharmacol. Rev. 59*, 5–13.

26. Gupta, A., Decaillot, F. M., and Devi, L. A. (2006) Targeting opioid receptor heterodimers: strategies for screening and drug development. *AAPS J. 8*, E153–E159.

27. Mirzadegan, T., Benko, G., Filipek, S., and Palczewski, K. (2003) Sequence analyses of G-protein-coupled receptors: similarities to rhodopsin. *Biochemistry 42*, 2759–2767.

28. Ballesteros, J. A., Jensen, A. D., Liapakis, G., Rasmussen, S. G., Shi, L., Gether, U., and Javitch, J. A. (2001) Activation of the beta 2-adrenergic receptor involves disruption of an ionic lock between the cytoplasmic ends of transmembrane segments 3 and 6. *J. Biol. Chem. 276*, 29171–29177.

29. Huang, P., Visiers, I., Weinstein, H., and Liu-Chen, L.-Y. (2002) The local environment at the cytoplasmic end of TM6 of the mu opioid receptor differs from those of rhodopsin and monoamine receptors: introduction of an ionic lock between the cytoplasmic ends of helices 3 and 6 by a L6.30(275)E mutation inactivates the mu opioid receptor and reduces the constitutive activity of its T6.34(279)K mutant. *Biochemistry 41*, 11972–11980.

30. Springael, J. Y., de Poorter, C., Deupi, X., Van Durme, J., Pardo, L., and Parmentier, M. (2007) The activation mechanism of chemokine receptor CCR5 involves common structural changes but a different network of interhelical interactions relative to rhodopsin. *Cell Signal. 19*, 1446–1456.

31. Bakker, R. A., Jongejan, A., Sansuk, K., Hacksell, U., Timmerman, H., Brann, M. R., Weiner, D. M., Pardo, L., and Leurs, R. (2007) Constitutively active mutants of the histamine H1 receptor suggest a conserved hydrophobic asparagine-cage that constrains the activation of class a GPCRs. *Mol. Pharmacol.*

32. Urizar, E., Claeysen, S., Deupi, X., Govaerts, C., Costagliola, S., Vassart, G., and Pardo, L. (2005) An activation switch in the rhodopsin family of G protein-coupled receptors: the thyrotropin receptor. *J. Biol. Chem. 280*, 17135–17141.

33. Park, P. S., Lodowski, D. T., and Palczewski, K. (2007) Activation of G protein-coupled receptors: beyond two-state models and tertiary conformational changes. *Annu. Rev. Pharmacol. Toxicol.*

34. Kjelsberg, M. A., Cotecchia, S., Ostrowski, J., Caron, M. G., and Lefkowitz, R. J. (1992) Constitutive activation of the alpha 1B-adrenergic receptor by all amino acid substitutions at a single site.

Evidence for a region which constrains receptor activation. *J. Biol. Chem. 267*, 1430–1433.

35. Mhaouty-Kodja, S., Barak, L. S., Scheer, A., Abuin, L., Diviani, D., Caron, M. G., and Cotecchia, S. (1999) Constitutively active alpha-1b adrenergic receptor mutants display different phosphorylation and internalization features. *Mol. Pharmacol. 55*, 339–347.

36. Gether, U., Lin, S., and Kobilka, B. K. (1995) Fluorescent labeling of purified beta 2 adrenergic receptor. Evidence for ligand-specific conformational changes. *J. Biol. Chem. 270*, 28268–28275.

37. Farrens, D. L., Altenbach, C., Yang, K., Hubbell, W. L., and Khorana, H. G. (1996) Requirement of rigid-body motion of transmembrane helices for light activation of rhodopsin. *Science 274*, 768–770.

38. Gether, U., Lin, S., Ghanouni, P., Ballesteros, J. A., Weinstein, H., and Kobilka, B. K. (1997) Agonists induce conformational changes in transmembrane domains III and VI of the beta2 adrenoceptor. *EMBO J. 16*, 6737–6747.

39. Davies, A., Gowen, B. E., Krebs, A. M., Schertler, G. F., and Saibil, H. R. (2001) Three-dimensional structure of an invertebrate rhodopsin and basis for ordered alignment in the photoreceptor membrane. *J. Mol. Biol. 314*, 455–463.

40. Marjamaki, A., Pihlavisto, M., Cockcroft, V., Heinonen, P., Savola, J. M., and Scheinin, M. (1998) Chloroethylclonidine binds irreversibly to exposed cysteines in the fifth membrane-spanning domain of the human alpha2A-adrenergic receptor. *Mol. Pharmacol. 53*, 370–376.

41. Marjamaki, A., Frang, H., Pihlavisto, M., Hoffren, A. M., Salminen, T., Johnson, M. S., Kallio, J., Javitch, J. A., and Scheinin, M. (1999) Chloroethylclonidine and 2-aminoethyl methanethiosulfonate recognize two different conformations of the human alpha(2A)-adrenergic receptor. *J. Biol. Chem. 274*, 21867–21872.

42. Ruprecht, J. J., Mielke, T., Vogel, R., Villa, C., and Schertler, G. F. (2004) Electron crystallography reveals the structure of metar-hodopsin I. *EMBO J. 23*, 3609–3620.

43. Jongejan, A., Bruysters, M., Ballesteros, J. A., Haaksma, E., Bakker, R. A., Pardo, L., and Leurs, R. (2005) Linking ligand binding to activation of the histamine H1 receptor. *Nat. Chem. Biol. 1*, 98–103.

44. Kobilka, B. (2004) Agonist binding: a multistep process. *Mol. Pharmacol. 65*, 1060–1062.

45. Chen, S., Lin, F., Xu, M., Riek, R. P., Novotny, J., and Graham, R. M. (2002) Mutation of a single TMVI residue, Phe(282), in the beta(2)-adrenergic receptor results in structurally distinct activated receptor conformations. *Biochemistry 41*, 6045–6053.

46. Abdulaev, N. G., and Ridge, K. D. (1998) Light-induced exposure of the cytoplasmic end of transmembrane helix seven in rhodopsin. *Proc. Natl. Acad. Sci. U.S.A. 95*, 12854–12859.

47. Elling, C. E., Thirstrup, K., Holst, B., and Schwartz, T. W. (1999) Conversion of agonist site to metal-ion chelator site in the beta(2)-adrenergic receptor. *Proc. Natl. Acad. Sci. U.S.A. 96*, 12322–12327.

48. Baranski, T. J., Herzmark, P., Lichtarge, O., Gerber, B. O., Trueheart, J., Meng, E. C., Iiri, T., Sheikh, S. P., and Bourne, H. R. (1999) C5a receptor activation. Genetic identification of critical residues in four transmembrane helices. *J. Biol. Chem. 274*, 15757–15765.

49. Pardo, L., Deupi, X., Dolker, N., Lopez-Rodriguez, M. L., and Campillo, M. (2007) The role of internal water molecules in the structure and function of the rhodopsin family of G protein-coupled receptors. *ChemBioChem. 8*, 19–24.

50. Fritze, O., Filipek, S., Kuksa, V., Palczewski, K.,,., Hofmann, K. P., and Ernst, O. P. (2003) Role of the conserved NPxxY(x)5,6F motif in the rhodopsin ground state and during activation. *Proc. Natl. Acad. Sci. U.S.A. 100*, 2290–2295.

51. Christoffers, K. H., Li, H., Keenan, S. M., and Howells, R. D. (2003) Purification and mass spectrometric analysis of the mu opioid receptor. *Brain Res. Mol. Brain Res. 118*, 119–131.

52. Chen, C., Xue, J. C., Zhu, J., Chen, Y. W., Kunapuli, S., de Riel, J. K., Yu, L., and Liu-Chen, L.-Y. (1995) Characterization of irreversible binding of beta-funaltrexamine to the cloned rat mu opioid receptor. *J. Biol. Chem. 270*, 17866–17870.

53. Chen, C., Yin, J., Riel, J. K., DesJarlais, R. L., Raveglia, L. F., Zhu, J., and Liu-Chen, L.-Y. (1996) Determination of the amino acid residue involved in [³H]beta-funaltrexamine covalent binding in the cloned rat mu-opioid receptor. *J. Biol. Chem. 271*, 21422–21429.